GRAPH-BASED TRACTOGRAPHY FOR ROBUST PROPAGATION THROUGH COMPLEX FIBRE CONFIGURATIONS

S. N. Sotiropoulos[1], L. Bai[2], P. S. Morgan[3,4], and C. R. Tench[1]

[1]Division of Clinical Neurology, University of Nottingham, Nottingham, United Kingdom, [2]School of Computer Science, University of Nottingham, Nottingham, United Kingdom, [3]Division of Academic Radiology, University of Nottingham, Nottingham, United Kingdom, [4]Radiology & Radiological Sciences, Medical University of South Carolina, Charleston, South Carolina, United States

Introduction

Tractography methods utilize diffusion-weighted (DW) MR images to reconstruct brain white matter tracts, non-invasively and in-vivo. Commonly used tractography techniques propagate curves within the vector fields of local fibre orientations [1, 2]. Alternatives to these streamline approaches have been developed based on graph theory, including fast marching [3, 4], shortest path [5] and fuzzy connectedness tractography [6]. These schemes are inherently discrete in the orientation and spatial fields. However, compared to the streamline schemes and their probabilistic counterparts, graph-based tractography combines a) converged indices of connectivity for all image voxels [3-6], b) connectivities that do not drop systematically with the distance from the seed [3-6], c) inherent ability to incorporate information from other imaging modalities [5] and d) relatively short execution times [6]. We present here a graph-based distributed tractography method that propagates robustly through voxels with complex fibre configurations, as these are depicted by the Q-ball orientation distribution functions (ODFs) [7].

Theory and Methods

Graph-based Tractography Theory: An image can be treated as a non-directed graph, with each voxel being a node in the graph and arcs connecting neighbouring voxels [5, 6]. Each arc is assigned a weight w_{ij} representing the probability of observing diffusion from voxel i to neighbouring voxel j, given the ODFs in these voxels. Weights can be calculated as the normalized integrals of the ODFs over a solid angle ϕ centred on the vector connecting i and j [5]. A path between any two voxels is a sequence of arcs connecting them. The strength of a path can be defined as the product of arc weights along its length. The strongest path connecting two voxels can then be found by exhaustively searching the image graph using, for example, Dijkstra's algorithm.

Limitations with Complex ODFs: The above approach works well with diffusion ODFs extracted from diffusion tensor imaging (DTI) [5]. However, there is an inherent problem when dealing with complex multiple-peak ODFs extracted from Q-ball data. In the example shown in Figure 1a, once a path reaches voxel A within the crossing region, it can equally likely propagate towards both crossing tracts, regardless of its origin. This can easily cause unrealistic path strengths and path propagation; note that the results of the ODF-driven fast marching tractography [4] will also be influenced by the same factor. The problem can be partially masked by the discrete nature of path propagation and the utilization of a maximum curvature threshold, as used in [5]. However, such threshold does not always work, as shown in the simple simulations of Figure 2a, where the strengths of the paths arising from a seed ROI within the horizontal tract are plotted for various crossing angles.

Multiple Voxel Instance Graph-based Tractography: In order to resolve such conditions, we assume that complex ODFs corresponding to N crossing populations can be decomposed to N simpler ODF components, each representative of a different population. Then, a voxel is represented in the image graph by N instances, one per population. Weights w_{ikjl} are defined between the k^{th} fibre population of voxel i and the l^{th} population of voxel j and are calculated by integrating the k^{th} and l^{th} ODF components of voxels i and j respectively. Using dynamic programming we test all the possible combinations and depending on the seed location let the appropriate ones dominate. For example, for the case of Figure 1a, the dominant configuration will be the one of Figure 1b (Figure 1c) if voxel B (voxel C) is used as a seed.

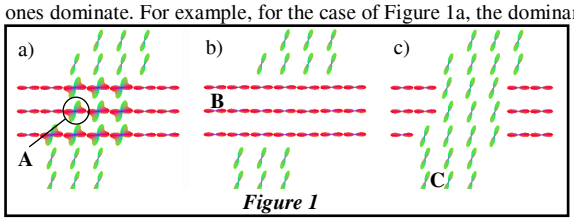

Figure 1

ODF Decomposition: We decompose the diffusion ODF using the deconvolution approach of [8]. A single fibre ODF kernel is calculated from the 300 most anisotropic voxels of the brain. Using this mean kernel, the diffusion ODF is deconvolved to a fibre ODF (fODF). The peaks of the fODF are determined using finite differences. Assuming that each peak n corresponds to a different crossing fibre population, the ODF kernel is rotated to the peak orientation to represent the n^{th} component of the original ODF. When only one peak is found, the original ODF is kept, thus allowing single-fibre fanning configurations that have a broader ODF to be treated appropriately.

Data Acquisition and Processing: Five healthy subjects that gave informed consent were scanned using a single-shot EPI DW sequence (in-plane resolution 2x2 mm^2, 2 mm slice thickness, parallel imaging factor=2) in a Philips 3T Achieva clinical imaging system. Six non-DW and 61 DW images [9] were acquired at b=3000 s/mm^2. Images were corrected for eddy current distortion and Q-ball ODFs were reconstructed using spherical harmonics (lmax=6) and Laplace-Beltrami regularization [8]. The graph weights were calculated using a 3x3x3 neighbourhood and a solid angle ϕ=2π/26. A maximum number of N=3 components were allowed in each voxel. All voxels with an FA>0.15 were considered for tractography.

Results and Discussion

Figure 2 presents simulated results for different crossing angles (60°-90°), when the graph-based tractography (GT) of [5] (Figure 2a) and the multiple voxel instance graph-based tractography with ODF decomposition (MVIGT) (Figure 2b) is used. The strengths of the paths arising from a seed ROI placed at the leftmost edge of the horizontal tract are plotted. The problem discussed above is evident especially for a 70° crossing, when mixing between the two tracts occurs. For a 60° crossing, due to increased perpendicular diffusivity, the ODF integration results to a higher weight for the diagonal neighbour than for the neighbour to the right. Therefore, the wrong tract is favoured. On the other hand, MVIGT propagates most strongly along the correct tract in all cases.

Figure 3 shows coronal maximum intensity projections of path strengths superimposed on FA maps, when a) GT and b) MVIGT are used with a seed ROI in the body of the corpus callosum (CC). Strengths smaller than 0.2 are cropped to aid visualization. We can observe how the specificity of the path strengths is increased through the crossings of the centrum semiovale and how the pyramidal tract paths are suppressed, when using MVIGT.

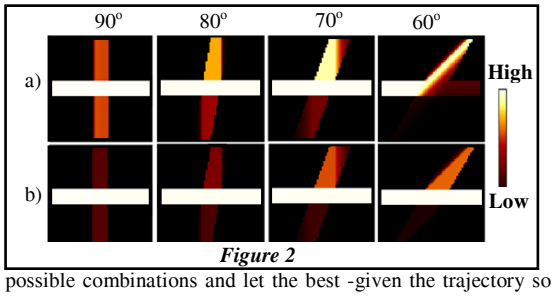

Figure 2

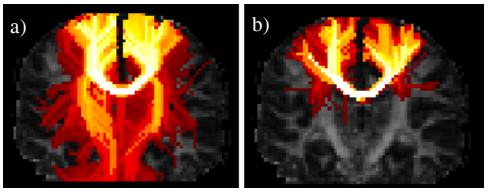

Figure 3

We have presented a distributed graph-based tractography method that robustly propagates through complex fibre configurations. Our method effectively borrows the idea of multi-tensor and Q-ball streamline tractography [10, 11], where in voxels with multiple orientations the one closest to the propagating trajectory is chosen. We apply a similar idea to graph-based tractography, without, however, having to select a fibre population. We instead try all the possible combinations and let the best -given the trajectory so far- dominate. In this implementation, we have used a common Gaussian ODF kernel throughout the brain. Even if the kernel is estimated from the data, we do not expect to be representative of all voxels. Different Gaussian kernels can be estimated on a voxel by voxel basis, by fitting multiple cylindrically symmetric tensors, as in [10, 12] and we are currently working towards this direction. Furthermore, fODF instead of diffusion ODF kernels can be used, the former being more representative of the actual fibre configurations [8].

References: **[1]** Basser et al, Magn Res Med, 2000 **[2]** Behrens et al, Magn Res Med 2003 **[3]** Parker et al, IEEE Trans Med Imag 2002 **[4]** Campbell et al, NeuroImage 2005 **[5]** Iturria-Medina et al, NeuroImage 2007 **[6]** Sotiropoulos et al, IEEE BIBE 2008 **[7]** Tuch, Magn Res Med, 2004 **[8]** Descoteaux et al, IEEE Trans Med Imag, 2008 **[9]** Cook et al, J Magn Res Imag 2007 **[10]** Parker & Alexander, IPMI 2003 **[11]** Seunarine et al, IEEE ICCV 2007 **[12]** Sotiropoulos et al, J Magn Res Imag 2008

Acknowledgement: This study is sponsored by the European Commission Fp6 Marie Curie Action programme (MEST-CT-2005-021170), under the CMIAG project.